JACS
JOURNAL OF THE AMERICAN CHEMICAL SOCIETY
Article
pubs.acs.org/JACS

Epitope-distal Effects Accompany the Binding of Two Distinct Antibodies to Hepatitis B Virus Capsids

Jessica Z. Bereszczak,[†,‡] Rebecca J. Rose,[†,‡,§] Esther van Duijn,[†,‡,#] Norman R. Watts,[∥] Paul T. Wingfield,[∥] Alasdair C. Steven,[⊥] and Albert J. R. Heck*[,†,‡]

[†]Biomolecular Mass Spectrometry and Proteomics, Bijvoet Center for Biomolecular Research and Utrecht Institute of Pharmaceutical Sciences, Utrecht University, Padualaan 8, 3584 CH, Utrecht, The Netherlands

[‡]The Netherlands Proteomics Centre, The Netherlands

[⊥]Laboratory of Structural Biology and [∥]Protein Expression Laboratory, National Institute for Arthritis, Musculoskeletal and Skin Diseases, National Institutes of Health, Bethesda Maryland 20892, United States

Supporting Information

ABSTRACT: Infection of humans by hepatitis B virus (HBV) induces the copious production of antibodies directed against the capsid protein (Cp). A large variety of anticapsid antibodies have been identified that differ in their epitopes. These data, and the status of the capsid as a major clinical antigen, motivate studies to achieve a more detailed understanding of their interactions. In this study, we focused on the Fab fragments of two monoclonal antibodies, E1 and 3120. E1 has been shown to bind to the side of outward-protruding spikes whereas 3120 binds to the "floor" region of the capsid, between spikes. We used hydrogen−deuterium exchange coupled to mass spectrometry (HDX-MS) to investigate the effects on HBV capsids of binding these antibodies. Conventionally, capsids loaded with saturating amounts of Fabs would be too massive to be readily amenable to HDX-MS. However, by focusing on the Cp protein, we were able to acquire deuterium uptake profiles covering the entire 149-residue sequence and reveal, in localized detail, changes in H/D exchange rates accompanying antibody binding. We find increased protection of the known E1 and 3120 epitopes on the capsid upon binding and show that regions distant from the epitopes are also affected. In particular, the α2a helix (residues 24−34) and the mobile C-terminus (residues 141−149) become substantially less solvent-exposed. Our data indicate that even at substoichiometric antibody binding an overall increase in the rigidity of the capsid is elicited, as well as a general dampening of its breathing motions.

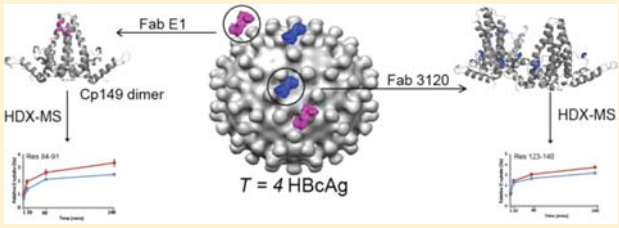

INTRODUCTION

The structural complexity and dynamic nature of multiprotein assemblies present a major challenge to comprehensive characterization. X-ray crystallography and cryo-electron microscopy provide detailed structural information but little direct insight into dynamic properties. NMR spectroscopy is more suited to monitoring dynamic structures in solution but is limited to relatively small particles. Hydrogen−deuterium exchange (HDX) provides information of a dynamic nature that can be assigned to specific regions of the protein.[1,2] When used in conjunction with mass spectrometry (MS),[3] hydrogen−deuterium exchange (HDX-MS) has the ability to interrogate complex systems at very low concentrations, providing incisive information on protein dynamics.[4−7]

HDX relies on the exchange of a protein's hydrogen atoms for a solvent's deuterium atoms.[8,9] The kinetics of exchange depend on exposure to solvent and hence on an atom's location in the protein and the protein's conformation and involvement in intramolecular hydrogen bonds; pH and temperature also affect the rate of exchange. Although hydrogen atoms involved in amino acid side chains are exchangeable, their exchange rates are too fast to be measured by MS, whereas amide hydrogen atoms in a protein backbone have exchange rates compatible with the time frame of a MS experiment. In the past decade, HDX-MS has benefited substantially from hardware and software developments, extending its reach beyond the characterization of small proteins to multidomain proteins and assemblies including, as in this study, antibodies bound to viral capsids. Applications have included: monitoring conformational changes induced by ligand-binding;[10−16] probing antibody−antigen interactions;[17,18] identification of protein−protein interfaces;[19,20] and protein unfolding/refolding.[21−24] Applications to viral processes have included: capsid assembly and maturation of human immunodeficiency virus (HIV);[25−27] maturation of bacteriophage P22;[28] pH-induced transitions in brome mosaic virus (BMV);[29] and structural analysis of the human rhinovirus (HRV14).[30]

In this study, we focus on capsids of hepatitis B virus (HBV) which assemble in two icosahedrally symmetric forms,

Received: December 14, 2012
Published: April 5, 2013

   dx.doi.org/10.1021/ja402023x | J. Am. Chem. Soc. 2013, 135, 6504−6512

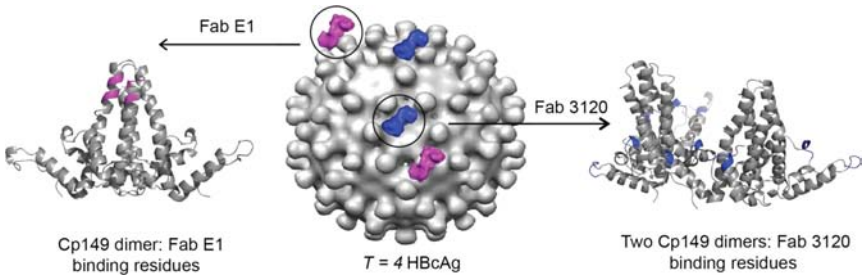

Figure 1. Interaction of Fab E1 (pink) and Fab 3120 (blue) with the $T = 4$ HBcAg capsid. Fab E1 binding residues are located near the spike and correspond to a discontinuous epitope (residues 70, 73, 74, 82, 83, 86, 87).[45] Fab 3120 binding residues correspond to a discontinuous epitope at the floor of the capsid and spans two adjacent dimeric subunits (A20−22, A25−29, A126−127 and B20−22, B129−132).[46]

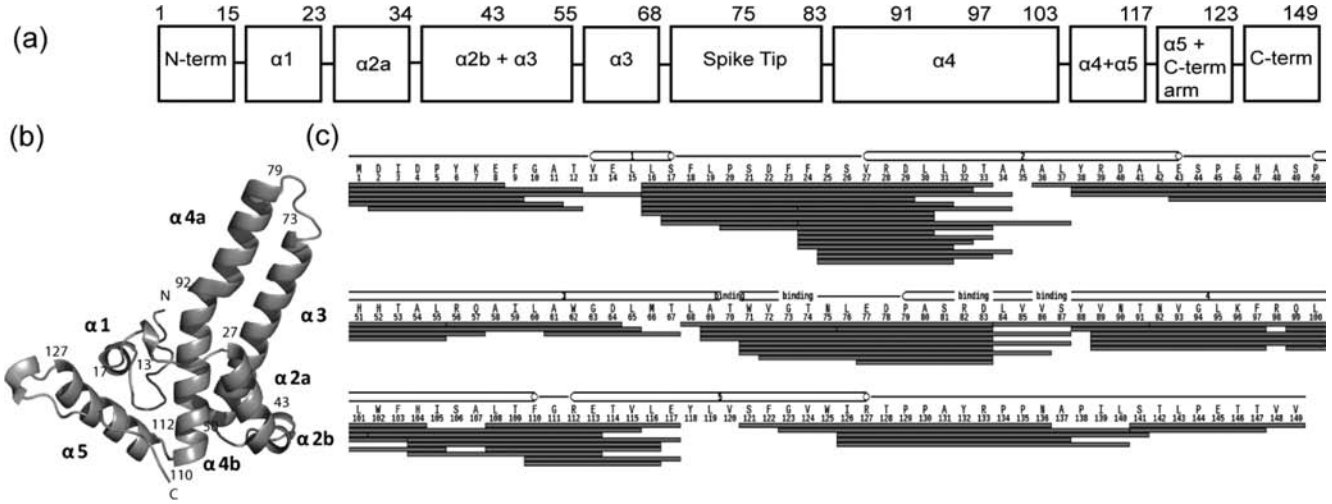

Figure 2. (a) Schematic to illustrate the structural components (and corresponding amino acid residues) constituting the HBV monomer. (b) Crystal structure of a HBV capsid monomer (PDB: 1QGT) indicating the different α-helices. (c) Experimentally observed sequence coverage of Cp149.3CA in which all peptides were observed in both nondeuterated and deuterated unbound HBcAg and Fab E1-bound HBcAg. A total of 67 peptides were identified leading to 98% sequence coverage (prepared using ref 73).

corresponding to triangulation numbers $T = 4$ and $T = 3$ and consisting of 240 and 180 subunits, respectively.[31] These capsids are known as hepatitis B core antigen (HBcAg). The building-blocks are dimers stabilized by an intermolecular four-helix bundle formed from two α-helical hairpins.[32−34] These bundles protrude as 25 Å-long spikes from the contiguous floor of the capsid (Figure 1). The native Cp monomer (Cp183) is 183 amino acids long and consists of an assembly domain (res. 1−149) (Figure 2a and b) and an Arg-rich C-terminal domain (res. 150−183). Many *in vitro* studies use, as we do here, the assembly domain (Cp149).[34−36]

Interaction of HBcAg with ten different monoclonal antibodies has been investigated by cryo-EM and the epitopes defined.[37−43] All but one of them are conformational. E1 is an especially important antibody because of its association with acute liver failure (ALF), the mechanism of which is largely unknown.[44] However, it has been shown that HBV-induced ALF is characterized by an overwhelming B-cell response, overproduction of antibodies and catastrophic liver damage.[44] Cryo-EM of Fab E1-decorated capsids localized the epitope to two neighboring helical motifs on the hairpin (res. 70−74 and 82−87) on one side of the spike[45] (Figure 1). Of note, the symmetry-related site on the other side of the spike remained unlabeled. Cryo-EM measurements indicated a Fab E1 binding stoichiometry, at saturation, of 36 Fab E1 to the $T = 3$ capsid, and 48 Fab E1 to the $T = 4$ capsid, representing only a 40% occupancy in comparison to the number of available spikes.[45]

In contrast, Fab 3120 binds to the capsid floor, where its epitope spans the interface between adjacent dimers, involving a total of five peptides (two copies each of two peptides and one copy of a third)[46] (Figure 1). At saturation, cryo-EM measurements indicated substoichiometric binding of 24 Fab 3120 to the $T = 3$ capsid, and 72 Fab 3120 to the $T = 4$ capsid.[46] The substoichiometric nature of both bindings is due in part to steric interference effects and in part to quasi-equivalent variations in the epitopes that affect the binding affinity. There may also be allosteric effects transmitted by the first few Fabs to bind, an aspect that is addressed further in the present study.

Here we use HDX-MS to further probe the interactions of Fabs E1 and 3120 with HBcAg. We show, at peptide level resolution, that several regions of the viral capsid undergo increased protection upon Fab binding, allowing us to discuss our data in the context of direct and indirect effects that Fab binding has on HBcAg structure.

METHODS

Preparation of HBcAg Capsids and Fab Fragments, and Decoration of Capsids with Fab. The Cp149.3CA consists of residues 1−149 with cysteines at positions 48, 61, and 107 changed to alanines. Cp149.3CA dimeric construct (abbreviated to Cp149 dimer) was purified as previously described.[36] Assembly into intact capsids was achieved via buffer exchange into an aqueous ammonium acetate buffer (200 mM) at pH 6.8 using an Amicon Ultra 0.5 mL centrifugal

dx.doi.org/10.1021/ja402023x | J. Am. Chem. Soc. 2013, 135, 6504−6512

filter (Millipore, Billerica, MA) with a molecular weight cutoff of 5 kDa. Expression and purification of Fab E1 has been previously described.[47] Monoclonal antibody (Fab 3120) was purchased from the Institute of Immunology, Tokyo, Japan and purified as previously described.[46] Both Fab fragments were buffer exchanged as described above. Decoration of capsids with Fab E1 was achieved by mixing Fab E1 with HBcAg to obtain a relative ratio of Cp149 dimer:Fab E1 (light chain, heavy chain) 1:2. In the case of Fab 3120, a Cp149 dimer:Fab 3120 ratio of 1:2.2 was used. These ratios ensured binding saturation. We also investigated the effect of substoichiometric binding of these Fab fragments to HBcAg at relative ratios of Cp149 dimer:Fab E1 of 2:1 and 4:1.

Hydrogen–Deuterium Exchange Mass Spectrometry (HDX-MS). A 30-fold dilution with either H_2O, pH 7 for the nondeuterated experiments, or deuterium oxide (Sigma Aldrich, Germany), pD 7 for deuterated experiments was carried out for the following complexes; unbound HBcAg (1 μL of 30 pmol/μL (Cp149 dimer concentration) into H_2O or D_2O), saturated Fab E1-bound HBcAg (1 μL of 30 pmol/μL HBcAg and 2 μL of 30 pmol/μL Fab E1 into H_2O or D_2O), Fab 3120-bound HBcAg (30 pmol of HBcAg and 65 pmol of Fab 3120), Fab E1-bound HBcAg at a relative ratio of Cp149 dimer:Fab E1 of 2:1 (30 pmol of HBcAg and 15 pmol of Fab E1) and 4:1 (30 pmol of HBcAg and 7.5 pmol of Fab E1). Diluted samples were incubated at room temperature for time intervals of 0 min for the nondeuterated experiments and 1, 10, 60, and 240 min for the deuterated experiments. While longer exposure times were investigated (22 h), the extent of the increase in deuterium incorporation did not warrant the added analysis time. The deuteration reaction was quenched by pH reduction to 2.5 with a 1:1 dilution using ice cold 4 M guanidine hydrochloride adjusted to pH 1.85, leading to an overall sample volume of 60 μL. Quenched samples at a final Cp149 dimer concentration of 0.5 pmol/μL were immediately injected into a 50 μL injection loop on a nano-ACQUITY UPLC system with HDX technology[48] (Waters Corporation, Milford, MA). Online digestion was performed using an immobilized pepsin column with 0.05% formic acid in H_2O, (flow rate of 200 μL/min), held at a temperature of 15 °C. Peptides were trapped and desalted online using an ACQUITY UPLC BEH C18 1.7 μm VanGuard Precolumn (Waters) at 0 °C, with subsequent elution onto an ACQUITY UPLC BEH C18 1.7 μm, 1 mm × 100 mm column (Waters) held at 0 °C. Peptide separation utilized a 8 min linear acetonitrile gradient (5–85%) containing 0.1% formic acid (flow rate of 40 μL/min). The eluent was directed into a Xevo G2 instrument (Waters) with electrospray ionization and lock-mass correction (using leu-enkephalin peptide). Mass spectra were acquired in MS^E mode over the m/z range 50–2000. Two blank injections were preformed between each sample injection to prevent sample carry over. Peptides were identified from the nondeuterated sample using ProteinLynx Global Server 2.5 software (Waters) and a databank containing the Cp149.3CA sequence. Wide search tolerances were used to increase the number of possible peptide candidates (e.g., search criteria of maximum number of peptides with minimum fragment ions, per peptide set to 2, and per protein set to 5).

Calculation of Exchange Data. Deuterium uptake was calculated and compared to the nondeuterated sample using DynamX 1.0.0 software (Waters), for the peptide candidates generated using the ProteinLynx Global Server. Only peptides observed in both the nondeuterated and deuterated samples were considered further. Experiments were carried out in triplicate at each time point with the exception of the Fab 3120 binding which, due to sample availability, was a single experiment. Measurements on Fab E1-bound complexes below saturation were carried out in duplicate. Absolute deuterium incorporation at a given time point was determined by comparison with $t = 0$ in the nondeuterated sample. The deuterium incorporation at a given time point corresponded to the centroid value across the backbone amide population. Results were averaged across replicate analyses at a given time point and the standard deviation determined. To examine the differences in a comparable way, the absolute deuterium uptake for each peptide (D uptake (Da)) was converted to a percentage deuterium uptake (% D) using eq 1, which

$$\%\ D = \frac{\text{D uptake (Da)}}{(\#aa's - N\text{-term.} - \#Pro)} \quad (1)$$

takes into consideration the total number of amino acids in the peptide (#aa's), the fast back exchange of hydrogens on the N-terminus (N-term.) and the lack of deuterium exchange of proline residues (#Pro).

Due to the unavoidable presence of "back exchange", it is preferable to assess the relative deuterium uptake between two states instead of the absolute deuterium uptake. The difference in the % deuterium uptake for Fab-bound HBcAg compared to unbound HBcAg, for a given peptide, gives the relative difference in deuterium uptake between the two states. Differences were considered significant if the value was greater than the sum of the standard deviations associated with both the unbound HBcAg and Fab E1-bound HBcAg (Tables S2 and S3, Supporting Information). Further testing of the results employed a t test to assign significance. Resulting p-values are given in Tables S2 and S3, Supporting Information, whereby a $p \geq 0.05$, was generally observed for all discussed changes. In the case of Fab 3120 binding, significance was ascribed to peptides whose deuterium uptake exceeded twice the standard deviation associated with the unbound HBcAg. Peptides were selected for comparison between the two states to ensure maximum sequence coverage and to be representative of other peptides covering a similar sequence.

Assessing the Extent of Back Exchange. A 60-fold dilution with either H_2O, pH 7 for the nondeuterated experiments, or deuterium oxide (Sigma Aldrich, Germany), pD 7 for deuterated experiments was carried out for a mixture of peptides consisting of bradykinin (188.4 μM), angiotensin (154.2 μM), glu-fibrinopeptide (12.8 μM) and leu-enkephalin (143.8 μM). The mixture was incubated at room temperature for 48 h and quenched and analyzed as described for HBcAg. The extent of deuteration of each peptide was determined as discussed for HBcAg. By comparison with the theoretical number of exchangeable amide bond hydrogens, the extent of amide backbone back exchange was determined, and estimated at ~30%.

Native Mass Spectrometry. High resolution mass spectra were recorded on a modified Q-ToF I instrument (Waters, Manchester, UK) in positive ion mode.[49] Xenon was used as the collision gas to increase the transmission of the HBcAg-Fab complexes,[50] and voltages and other gas pressures optimized for the transmission of large noncovalent protein complexes.[51,52] Briefly, the capillary and cone voltages were kept constant at 1250 and 150 V, respectively. The voltage before the collision cell (collision energy (CE)) was varied between 100 and 150 V for MS analysis. Ions were introduced into the source at an increased pressure of 10 mbar. For unbound HBcAg (analyzed at 4 μM Cp149 dimer concentration), charge state resolution was observed, and masses were determined for all detected ions in the charge state distribution. For Fab E1-bound HBcAg complexes, charge state resolution was not obtained hence the m/z at maximum ion intensity for the $T = 3$ and $T = 4$ distributions was determined by multipeak fitting of two Gaussian-type distributions using the software IGORPro.[53]

RESULTS

HDX-MS of the HBcAg Capsid. LC-MS^E analysis of pepsin-digested HBcAg identified a total of 67 peptides, many of which were partially overlapping, covering 98% of the Cp sequence (Figure 2c). Deuterium exchange of backbone amide hydrogens was carried out for exposure times of 1 min, 10 min, 60 and 240 min, and the relative deuterium uptake compared to time zero ($t = 0$) for each peptide was determined. To understand how the structure of the HBcAg capsid affects the relative exposure of the different amide hydrogens, the deuterium uptake (as % deuterium uptake per peptide) at the different time points was compared (Table S1, Supporting Information). Peptides that show the highest levels of deuterium incorporation correspond to the α2a helix (peptide 24–34), the dimeric spike tip (peptides 69–75, 76–83, 84–91

dx.doi.org/10.1021/ja402023x | J. Am. Chem. Soc. 2013, 135, 6504–6512

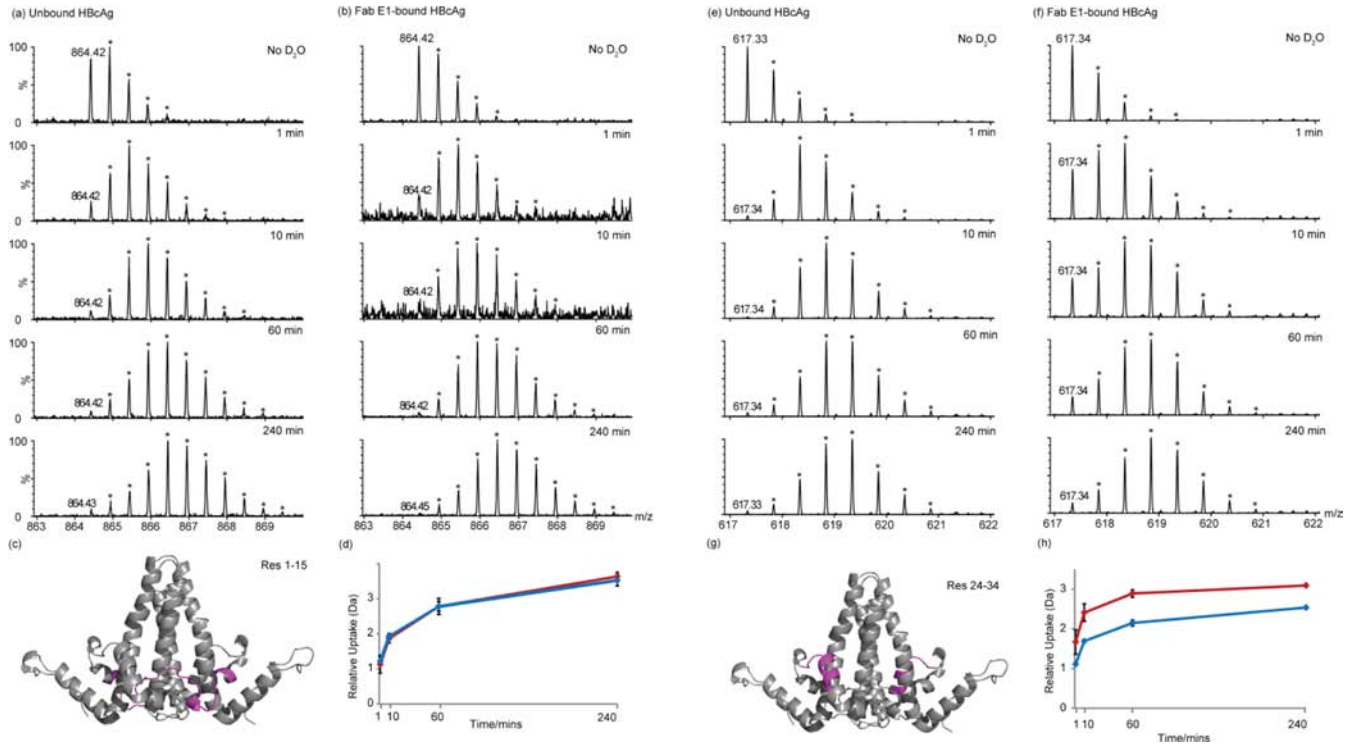

Figure 3. Differential deuterium uptake of unbound HBcAg and Fab E1-bound HBcAg for peptides comprising residues 1−15 (a−d) and residues 24−34 (residues e−h). The peptide at m/z 864.4 corresponding to residues 1−15 (c) is observed in nondeuterated unbound HBcAg (a) and in nondeuterated Fab E1-bound HBcAg (b). The deuterium uptake is monitored at different exposure times; 1 min, 10 min, 60 and 240 min. The deuterium uptake relative to $t = 0$ can be determined (d) for both unbound HBcAg (red) and Fab E1-bound HBcAg (blue). Similarly, the peptide at m/z 617.3 corresponding to residues 24−34 (g) is observed in nondeuterated unbound HBcAg (e) and in nondeuterated Fab E1-bound HBcAg (f). The deuterium uptake relative to $t = 0$ can be determined (h) for both the unbound HBcAg (red) and Fab E1-bound HBcAg (blue). In all cases the m/z of the monoisotopic ion is indicated, with the other ions constituting the distribution indicated with *.

and 89−97) and the C-terminus (peptide 141−149), and at the maximum exposure time (240 min), the % deuterium uptake ranges from 34−65%. Peptides with lower levels of deuteration correspond to the N-terminus (peptide 1−15) and those involved in the numerous α-helices, namely, the α1 helix (peptide 16−23), the α2b helix plus the α3 helix (peptides 36−43 and 44−55), the α3 helix (peptide 55−64 and 61−67), the α4b helix (peptide 89−103), the α4b helix plus the α5 helix (peptide 104−117) and the α5 helix plus the C-terminal arm (peptide 123−140) (Figure 2b). Additional confidence in the results was confirmed by comparison with a second data set (also constituting three repeat measurements). The root-mean square difference between the two data sets was approximately 4%.

Effect of Fab E1 Binding on HBcAg Structure. To evaluate the conformational changes induced by Fab E1 binding, the deuterium uptake was monitored for all observed peptides at the various time points, using an antibody concentration consistent with saturation binding to HBcAg (Table S2, Supporting Information). Two types of distributions at the peptide level were observed; those in which Fab binding did not alter the level of deuterium uptake, and those in which the deuterium incorporation significantly decreased upon Fab binding. An example in which Fab E1 binding had minimal effect on deuterium uptake compared to unbound HBcAg, involves the peptide covering residues 1−15 (Figure 3c). Monitoring the deuterium uptake for the nondeuterated $[M + 2H]^{2+}$ ion at m/z 864.4 in both the unbound HBcAg (Figure 3a) and the Fab E1-bound HBcAg (Figure 3b), indicated minimal difference in deuterium incorporation between the two states (Figure 3d). In contrast, a clear reduction in deuterium incorporation upon Fab E1 binding was observed for the peptide spanning residues 24−34 (the α2a helix) (Figure 3g). Monitoring the deuterium uptake for the nondeuterated $[M + 2H]^{2+}$ ion at m/z 617.3 in both the unbound HBcAg (Figure 3e) and the Fab E1-bound HBcAg (Figure 3f), indicated a significant reduction in deuterium incorporation upon Fab E1 binding (Figure 3h).

A representation of the conformational changes in HBcAg induced by Fab E1 binding was made by mapping the difference in % deuterium uptake between the two states as a color change on the Cp149 dimer (PDB: 1QGT) (Figure 4). In all cases where a substantial difference between the two states was observed, Fab E1 binding led to a reduction in deuterium incorporation upon binding. At the longest exchange time (240 min), regions showing a significant reduction in deuterium uptake upon Fab E1 binding were restricted to the regions comprising residues 24−34, 69−75, 76−83, 84−91, 89−97, 89−103 and 141−149. In all cases, the difference was between 4.4 and 13.3% per peptide. All other regions showed no significant difference in deuterium incorporation upon Fab E1 binding Figure S1, Supporting Information). The largest reductions in deuterium uptake upon binding were observed for; peptide 84−91 (the spike tip and cryo-EM-identified epitope) with a 13.3% reduction, peptide 141−149 (C-terminus) with a 9.2% reduction and peptide 24−34 (α2a helix) with a 5.8% reduction.

dx.doi.org/10.1021/ja402023x | J. Am. Chem. Soc. 2013, 135, 6504−6512

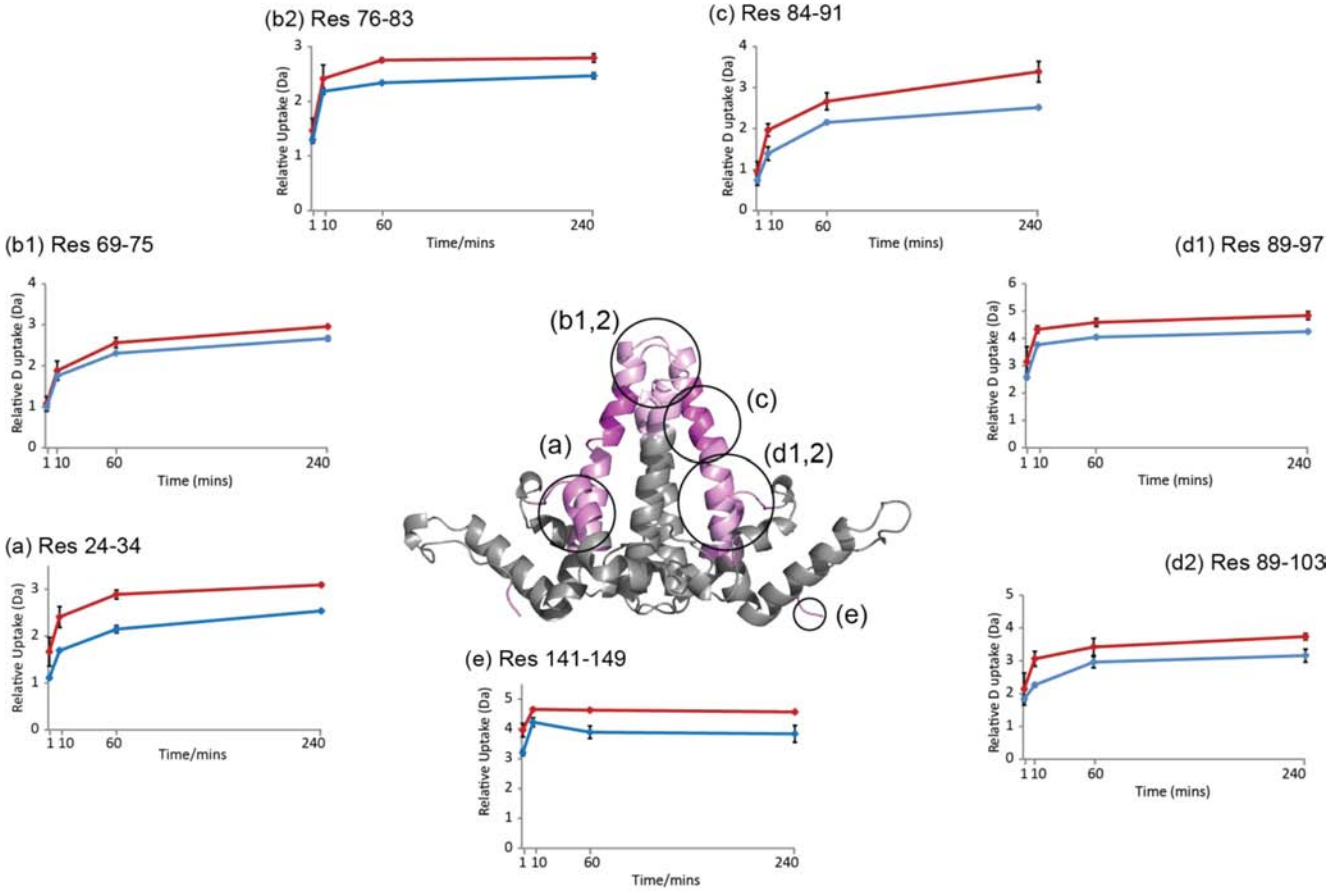

Figure 4. Significant reduction in deuterium uptake upon Fab E1 binding is visualized as a color change on the crystal structure of the Cp149 dimer (t = 240 min). Gray represents the structural regions where there is no significant difference in deuterium incorporation between unbound and Fab E1-bound states, with increasing intensity of pink representing a greater reduction in deuterium uptake upon binding. Typical individual relative deuterium uptake versus exposure time graphs for both the unbound HBcAg (red) and the Fab E1-bound HBcAg (blue) are also shown for regions of the structure showing significant reductions in deuterium incorporation upon binding.

HBcAg-Fab E1 complexes at substoichiometric binding conditions (HBcAg/Fab E1 of 2:1 and 4:1) were also investigated to examine the effect on HBcAg structure of binding only a few Fabs. Native mass spectrometry confirmed that at lower Fab concentrations HBcAg binds a reduced number of Fab E1 (Figure S2, Supporting Information). Cryo-EM data has indicated that at saturation the T = 3 capsid binds 36 Fab E1 (out of 90 possible spike epitopes, assuming only one viable epitope per dimeric spike) and the T = 4 capsid binds 48 Fab E1 (out of 120 epitopes). Using these data and the mass spectra corresponding to the lower binding ratio complexes, we estimate that at a HBcAg/Fab E1 of 2:1 15 Fab E1 bind to the T = 3 capsid and 24 Fab E1 bind to the T = 4 capsid, and at a relative ratio of 4:1 less than 5 copies of Fab E1 bind to either T = 3 and T = 4 capsids. Monitoring the deuterium uptake of these complexes revealed that even at the lowest binding ratio a reduction in deuterium uptake was observed for the α2a helix and the C-terminus (Figure S3, Supporting Information), suggesting that suppression of breathing motion is already induced upon binding of just a few Fabs.

Effect of Fab 3120 Binding on HBcAg Structure. To reveal the conformational changes induced by Fab 3120 binding, the deuterium uptake was monitored for all observed peptides at the different time points, again at an antibody concentration representing binding saturation (Table S3, Supporting Information). At the longest time point (240 min), many regions showed a substantial reduction in deuterium uptake upon Fab 3120 binding except for residues 56−67 and 98−103 (Figure 5). This observed reduction in deuterium uptake amounted to 2 to 16.4% per peptide. The largest differences were observed for residues 24−34 (α2a helix), and residues 141−149 (the C-terminus), representing a 11.6 and a 16.4% decrease in deuterium uptake, respectively.

■ DISCUSSION

Exposure of the Capsid Protein within Unbound HBcAg. X-ray crystallography and cryo-EM have provided vital insights into the structure and subunit packing of HBV capsids, however a more complete picture would include the dynamic properties of this assembly, and the effects of interaction with anticapsid antibodies. HDX-MS affords a powerful method to study and localize conformational dynamics especially when the (static) high resolution structure is known. Prior to assessing the effects of antibody binding on the HBcAg structure, we discuss the HDX-MS-observed conformational dynamics of undecorated HBcAg capsids.

The high sequence coverage (98%) and profusion of peptides (67) observed upon pepsin digestion of HBcAg (Figure 2c) allowed us to map fully the dynamics within the capsid. The presence of multiple peptides representing overlapping regions demonstrate the consistency of the data

dx.doi.org/10.1021/ja402023x | J. Am. Chem. Soc. 2013, 135, 6504−6512

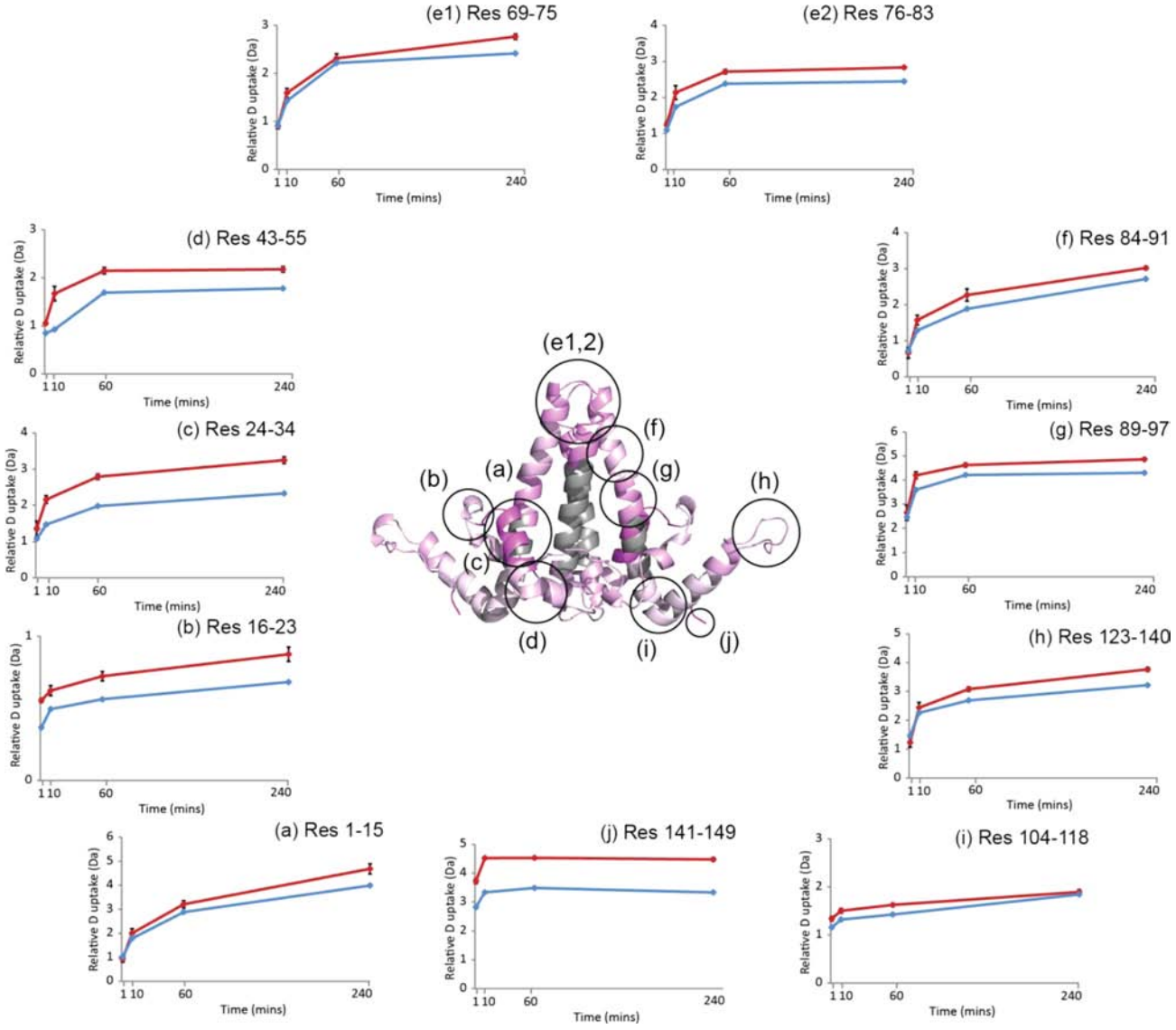

Figure 5. Significant reduction in deuterium uptake upon Fab 3120 binding is visualized as a color change on the crystal structure of the Cp149 dimer (t = 240 min). Gray represents the structural regions where there is no significant difference in the deuterium incorporation between the unbound and Fab 3120-bound states, with increasing intensity of pink representing a greater reduction in deuterium uptake upon Fab 3120 binding. Typical individual relative deuterium uptake versus exposure time graphs for both the unbound HBcAg (red) and the Fab 3120-bound HBcAg (blue) are also shown for the regions of the structure showing significant reductions in deuterium incorporation upon Fab 3120 binding.

and enhance confidence in the results. Examination of these peptides established that certain regions exhibit substantially different levels of accessibility to hydrogen exchange (Table S1, Supporting Information). Regions exhibiting the highest levels of deuterium exchange; the α2a helix (peptide 24−34), the spike tip (peptides 69−75, 76−83, 84−91 and 89−97) and the C-terminus (141−149) must represent exposed and/or flexible regions of the capsid, and consequently may be involved in breathing motions of the capsid. The high solvent accessibility of the spike tip is consistent with its location at the very periphery of the capsid. The α2a helix must also be flexible and dynamically exposed, which may reflect its minimal involvement in interdimer interactions. Of all observed peptides the C-terminus consistently showed the highest level of deuterium uptake at all exposure times (average 63% deuterium uptake across the time points). This high level of exposure is consistent with reports of the flexibility of the C-terminus and its transient exposure on the outer surface of empty capsids.[36,54−58]

The lower levels of deuterium uptake exhibited by other regions are likely to result from their locations at the capsid floor (peptides 36−43, 44−55 and 104−117), and in some cases, involvement in interdimer interactions (peptides 104−117 and 123−140) and thus confirm the higher level of structural protection afforded by the capsid shell. In addition, the extensive hydrogen bonding in the α-helices that make up the majority of HBcAg structure would also increase protection and lead to lower levels of deuterium incorporation (peptides 16−23, 36−43, 44−55, 55−64, 61−67, 89−103 and 104−117), especially those peptides (peptides 55−64 and 61−67) constituting the α3 helix which is involved in the extensive intersubunit contacts in the 4-helix bundle.

Conformational Changes Induced by Fab E1 Binding to HBcAg. In our investigation of conformational changes induced by Fab E1 binding to HBcAg we observed that much of the capsid protein shows little difference in deuterium incorporation between the unbound and Fab E1-bound states

dx.doi.org/10.1021/ja402023x | J. Am. Chem. Soc. 2013, 135, 6504−6512

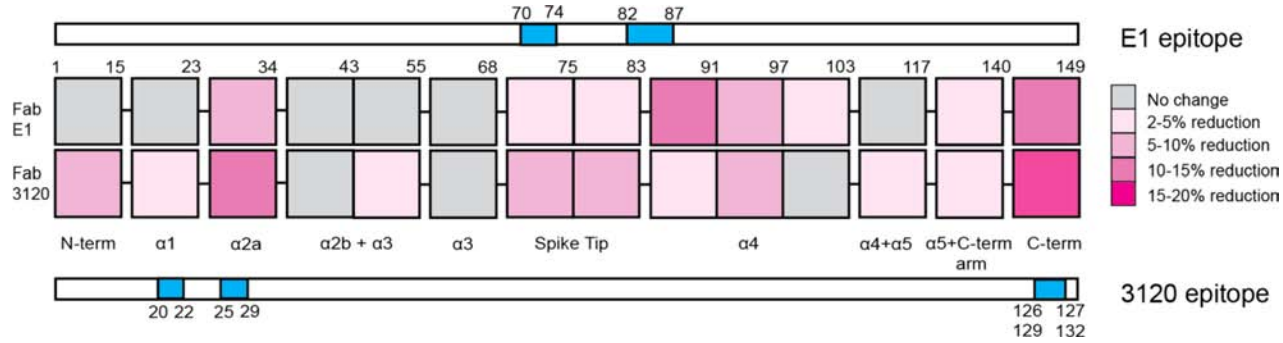

Figure 6. Significant reduction in deuterium uptake upon Fab binding to HBcAg (t = 240 min) is visualized as a color change on a schematic of the Cp149 sequence, for the binding of both Fab E1 and Fab 3120. The increasing intensity of pink represents a greater reduction in deuterium uptake upon Fab binding (derived by comparison of the % deuterium uptake for a given peptide between unbound and Fab-bound HBcAg).

(Table S2 and Figure S1, Supporting Information). In particular, these were identified as those regions closest to the capsid floor and those regions involved in interdimer interactions, and as such may demonstrate the already highly protected environment of the capsid shell. However, it is striking that the regions affected by Fab E1 binding include some that are quite remote from the peptides that make up the epitope (Figure 6) and all changes recorded involve reduced rates of exchange. As such, they point to a global rigidification of the capsid, that is, a suppression of its breathing motions (statistical fluctuations in structure).

The primary changes in exchange pattern upon binding Fab E1 can be pin-pointed to four regions all of which undergo increased protection (Figures 4 and 6, Figure S4a, , Supporting Information). They correspond to the α2a helix, the spike tip, the α4 helix and the C-terminus. The increased protection at the spike tip is consistent with the location of the E1 epitope as defined by cryo-EM (residues 70, 73, 74, 82, 83, 86, 87).[45] Peptide 84−91 undergoes the largest reduction in deuterium uptake, fully consistent with this assignment. Residues 91−103 directly follow this region and we can assume that the increased protection observed at the spike tip continues into this part of the α4 helix. Cryo-EM previously demonstrated that at saturation substoichiometric binding of Fab E1 leads to occupation of only 40% of the available spikes.[45] This may explain why we do not observe a larger reduction in deuterium uptake at the epitope as might be predicted from interaction of Fab E1 with all available spikes. Cryo-EM data did not observe a role for the α2a helix in Fab E1 binding, but our HDX-MS data shows that this region undergoes a considerable decrease in deuterium uptake, suggesting that conformational stabilization is transmitted allosterically to this site by Fab E1 binding to its epitope, resulting in reduced flexibility and increased protection. At lower Fab E1 binding stoichiometries (HBcAg/Fab E1 of 2:1 and 4:1) (Figure S2, Supporting Information) the deuterium uptake at regions distal to the epitope, the α2a helix and the C-terminus, were also reduced compared to the uptake of unbound HBcAg (Figure S3, Supporting Information). This strongly indicates that dampening of the HBV capsid flexibility already occurs upon binding of a few Fab E1.

A functional consequence of the conformational changes upon E1 binding to the dimeric capsid protein is that binding to the second epitope on either capsids or nonassembled dimers is blocked.[45] The site unavailable for binding must sense binding at the other site via transmitted conformational changes, as discussed above. In other systems, α-helices have been shown to move like rigid bodies during protein breathing and in the all-helical HBV capsids, a similar mechanism may mediate dynamic structural changes at a distance.[59]

Conformational Changes Induced by Fab 3120 Binding to HBcAg. The potential of this methodology led us to also investigate the binding of Fab 3120 that has been shown by cryo-EM to bind to an interdimer interface region on the capsid floor[46]- a very different location from the E1 epitope. A comparison of the hydrogen exchange patterns between the unbound HBcAg and Fab 3120-bound HBcAg (Table S3, Supporting Information) again revealed many differences (Figures 5 and 6, Figure S4b, Supporting Information). The extent of protection however, was in a similar range (2−16% per peptide) to those observed upon Fab E1 binding. Similarly, when a change in deuterium uptake was observed, it was a reduction. Consistent with Fab E1 binding, Fab 3120 binding to HBcAg showed both the α2a helix and the C-terminus as undergoing the largest reduction in deuterium uptake, suggesting that these conformational changes are independent of the type of Fab that binds, although the extent of reduction in deuterium uptake differed between the two Fabs (Figure 6). Considering the location of the Fab 3120 epitope on the capsid floor (Figure 1), a number of steric considerations arise; in particular, the Fab has to fit between adjacent spikes. Moreover, the greater size of the footprint on the capsid surface would imply that binding of this Fab could result in increased protection to a larger expanse of the capsid structure compared to a spike-binding Fab. Our HDX-MS data are consistent with this proposition.

Fab Binding Suppresses Breathing of the Capsid. A notable dynamic property that has been observed for several viral capsids is their ability to transiently expose to the outside amino acid sequences that normally reside in the interior. This behavior, which takes place under physiological conditions, is termed "breathing". To date, it has been observed in poliovirus,[60−62] human rhinoviruses HRV14[63,64] and HRV16,[64] tetraviruses, for example, *Nudaurelia ω capensis* (NωV) and *Helicoverpa armigera* stunt virus (HaSV),[65] nodaviruses, for example, flock house virus[66] and bromoviruses, for example, *cowpea chlorotic mottle virus* (CCMV).[67]

Per HBcAg, the location and role of the 34-residue C-terminal region of Cp183 has received considerable attention. Early work identified the importance of this Arg-rich domain in the binding of the RNA pregenome (Cp183), an assignment confirmed by EM labeling studies.[31,35,68−71] On the other hand, proteolysis data suggested accessibility of the C-terminal domain to proteases,[54−56] and foreign sequences inserted at

dx.doi.org/10.1021/ja402023x | J. Am. Chem. Soc. 2013, 135, 6504−6512

the C-terminus retained immunogenicity.[57,58] A more recent study documented the binding of kinase SRPK to the C-terminus on the external surface of empty Cp183 constructs.[72] These data attest to the dynamic nature of this domain and its transient exposure to the capsid exterior. The present observations suggest that binding of both Fab E1 and Fab 3120 has the overall effect of increasing the rigidity of the capsid and consequently dampening or suppressing its breathing. This dampening effect, in the case of Fab E1, is observed even at binding stoichiometries below saturation.

CONCLUSION

Here, HDX-MS has been shown to be a powerful technique for characterizing the dynamics of the HBcAg capsid and its interaction with antibodies. To our knowledge, this is the first time intact virus−antibody complexes, with estimated masses above 6 MDa,[45,46] have been probed using HDX-MS. These data have provided unique complementary insights into the conformational flexibility of the HBcAg capsid and how this property changes upon antibody binding. This information is difficult to assess by any other analytical technique, thus illustrating the unique potential of HDX-MS.

ASSOCIATED CONTENT

Supporting Information

Additional relative deuterium uptake versus deuterium exposure time graphs for unbound HBcAg and Fab E1-bound HBcAg at different relative ratios of HBcAg/Fab E1; native-MS of unbound HBcAg and Fab E1-bound HBcAg; table detailing the deuterium incorporation of selected peptides for unbound HBcAg at different deuterium exposure times, and graphs and tables corresponding to the difference in % deuterium incorporation between unbound HBcAg and Fab E1-bound HBcAg, and unbound HBcAg and Fab 3120-bound HBcAg for all observed peptides, at deuterium exposure times of 1, 10, 60 and 240 min. This material is available free of charge via the Internet at http://pubs.acs.org.

AUTHOR INFORMATION

Corresponding Author

a.j.r.heck@uu.nl

Present Addresses

[§]UCB Celltech, Slough, UK.
[#]TNO, Zeist, The Netherlands.

Notes

The authors declare no competing financial interest.

ACKNOWLEDGMENTS

This work was supported in part by The Netherlands Organization for Scientific Research (NWO) with ALW-ECHO (819.02.10) to A.J.R.H. and a VENI grant to E.v.D (700.58.402) and in part by the Intramural Research Program of NIAMS. We thank The Netherlands Proteomics Centre, embedded in The Netherlands Genomics Initiative, for financial support.

REFERENCES

(1) Engen, J. R. *Anal. Chem.* **2009**, *81*, 7870.
(2) Konermann, L.; Pan, J.; Liu, Y. H. *Chem. Soc. Rev.* **2011**, *40*, 1224.
(3) Katta, V.; Chait, B. T. *Rapid Commun. Mass Spectrom.* **1991**, *5*, 214.
(4) Zhang, Z.; Smith, D. L. *Protein Sci.* **1993**, *2*, 522.
(5) Smith, D. L.; Deng, Y.; Zhang, Z. *J. Mass Spectrom.* **1997**, *32*, 135.
(6) Wales, T. E.; Engen, J. R. *Mass Spectrom. Rev.* **2006**, *25*, 158.
(7) Morgan, C. R.; Engen, J. R. *Curr. Protoc. Protein Sci.* **2009**, *58*, 17.6.1.
(8) Hvidt, A.; Linderstrom-Lang, K. *Biochim. Biophys. Acta* **1954**, *14*, 574.
(9) Hvidt, A.; Nielsen, S. O. *Adv. Protein Chem.* **1966**, *21*, 287.
(10) Brier, S.; Lemaire, D.; DeBonis, S.; Kozielski, F.; Forest, E. *Rapid Commun. Mass Spectrom.* **2006**, *20*, 456.
(11) Houde, D.; Arndt, J.; Domeier, W.; Berkowitz, S.; Engen, J. R. *Anal. Chem.* **2009**, *81*, 2644.
(12) Kong, L.; Huang, C. C.; Coales, S. J.; Molnar, K. S.; Skinner, J.; Hamuro, Y.; Kwong, P. D. *J. Virol.* **2010**, *84*, 10311.
(13) Burkitt, W.; Domann, P.; O'Connor, G. *Protein Sci.* **2010**, *19*, 826.
(14) Marcsisin, S. R.; Narute, P. S.; Emert-Sedlak, L. A.; Kloczewiak, M.; Smithgall, T. E.; Engen, J. R. *J. Mol. Biol.* **2011**, *410*, 1008.
(15) Wei, H.; Ahn, J.; Yu, Y. Q.; Tymiak, A.; Engen, J. R.; Chen, G. *J. Am. Soc. Mass Spectrom.* **2012**, *23*, 498.
(16) Weinreb, P. H.; Li, S.; Gao, S. X.; Liu, T.; Pepinsky, R. B.; Caravella, J. A.; Lee, J. H.; Woods, V. L., Jr. *J. Biol. Chem.* **2012**, *287*, 32897.
(17) Baerga-Ortiz, A.; Hughes, C. A.; Mandell, J. G.; Komives, E. A. *Protein Sci.* **2002**, *11*, 1300.
(18) Coales, S. J.; Tuske, S. J.; Tomasso, J. C.; Hamuro, Y. *Rapid Commun. Mass Spectrom.* **2009**, *23*, 639.
(19) Mandell, J. G.; Falick, A. M.; Komives, E. A. *Proc. Natl. Acad. Sci. U.S.A.* **1998**, *95*, 14705.
(20) Yamada, N.; Suzuki, E.; Hirayama, K. *Rapid Commun. Mass Spectrom.* **2002**, *16*, 293.
(21) Miranker, A.; Robinson, C. V.; Radford, S. E.; Aplin, R. T.; Dobson, C. M. *Science* **1993**, *262*, 896.
(22) Engen, J. R.; Smithgall, T. E.; Gmeiner, W. H.; Smith, D. L. *Biochemistry* **1997**, *36*, 14384.
(23) Wani, A. H.; Udgaonkar, J. B. *Proc. Natl. Acad. Sci. U.S.A.* **2009**, *106*, 20711.
(24) Pan, J.; Han, J.; Borchers, C. H.; Konermann, L. *Anal. Chem.* **2010**, *82*, 8591.
(25) Lanman, J.; Lam, T. T.; Emmett, M. R.; Marshall, A. G.; Sakalian, M.; Prevelige, P. E., Jr. *Nat. Struct. Mol. Biol.* **2004**, *11*, 676.
(26) Cortines, J. R.; Monroe, E. B.; Kang, S.; Prevelige, P. E., Jr. *J. Mol. Biol.* **2011**, *410*, 641.
(27) Monroe, E. B.; Kang, S.; Kyere, S. K.; Li, R.; Prevelige, P. E., Jr. *Structure* **2010**, *18*, 1483.
(28) Tuma, R.; Coward, L. U.; Kirk, M. C.; Barnes, S.; Prevelige, P. E., Jr. *J. Mol. Biol.* **2001**, *306*, 389.
(29) Wang, L.; Lane, L. C.; Smith, D. L. *Protein Sci.* **2001**, *10*, 1234.
(30) Wang, L.; Smith, D. L. *Protein Sci.* **2005**, *14*, 1661.
(31) Crowther, R. A.; Kiselev, N. A.; Bottcher, B.; Berriman, J. A.; Borisova, G. P.; Ose, V.; Pumpens, P. *Cell* **1994**, *77*, 943.
(32) Bottcher, B.; Wynne, S. A.; Crowther, R. A. *Nature* **1997**, *386*, 88.
(33) Conway, J. F.; Cheng, N.; Zlotnick, A.; Wingfield, P. T.; Stahl, S. J.; Steven, A. C. *Nature* **1997**, *386*, 91.
(34) Wynne, S. A.; Crowther, R. A.; Leslie, A. G. *Mol. Cell* **1999**, *3*, 771.
(35) Wingfield, P. T.; Stahl, S. J.; Williams, R. W.; Steven, A. C. *Biochemistry* **1995**, *34*, 4919.
(36) Zlotnick, A.; Cheng, N.; Conway, J. F.; Booy, F. P.; Steven, A. C.; Stahl, S. J.; Wingfield, P. T. *Biochemistry* **1996**, *35*, 7412.
(37) Takahashi, K.; Machida, A.; Funatsu, G.; Nomura, M.; Usuda, S.; Aoyagi, S.; Tachibana, K.; Miyamoto, H.; Imai, M.; Nakamura, T.; Miyakawa, Y.; Mayumi, M. *J. Immunol.* **1983**, *130*, 2903.
(38) Ferns, R. B.; Tedder, R. S. *J. Med. Virol.* **1986**, *19*, 193.
(39) Petit, M. A.; Capel, F.; Riottot, M. M.; Dauguet, C.; Pillot, J. *J. Gen. Virol.* **1987**, *68* (Pt 11), 2759.
(40) Belnap, D. M.; Watts, N. R.; Conway, J. F.; Cheng, N.; Stahl, S. J.; Wingfield, P. T.; Steven, A. C. *Proc. Natl. Acad. Sci. U.S.A.* **2003**, *100*, 10884.

(41) Harris, A.; Belnap, D. M.; Watts, N. R.; Conway, J. F.; Cheng, N.; Stahl, S. J.; Vethanayagam, J. G.; Wingfield, P. T.; Steven, A. C. *J. Mol. Biol.* **2006**, *355*, 562.
(42) Watts, N. R.; Cardone, G.; Vethanayagam, J. G.; Cheng, N.; Hultgren, C.; Stahl, S. J.; Steven, A. C.; Sallberg, M.; Wingfield, P. T. *J. Mol. Biol.* **2008**, *379*, 1119.
(43) Kandiah, E.; Watts, N. R.; Cheng, N.; Cardone, G.; Stahl, S. J.; Heller, T.; Liang, T. J.; Wingfield, P. T.; Steven, A. C. *J. Struct. Biol.* **2012**, *177*, 145.
(44) Farci, P.; Diaz, G.; Chen, Z.; Govindarajan, S.; Tice, A.; Agulto, L.; Pittaluga, S.; Boon, D.; Yu, C.; Engle, R. E.; Haas, M.; Simon, R.; Purcell, R. H.; Zamboni, F. *Proc. Natl. Acad. Sci. U.S.A.* **2010**, *107*, 8766.
(45) Wu, W.; Chen, Z.; Cheng, N.; Watts, N. R.; Stahl, S. J.; Farci, P.; Purcell, R. H.; Wingfield, P. T.; Steven, A. C. *J. Struct. Biol.* **2013**, *18*, 53.
(46) Conway, J. F.; Watts, N. R.; Belnap, D. M.; Cheng, N.; Stahl, S. J.; Wingfield, P. T.; Steven, A. C. *J. Virol.* **2003**, *77*, 6466.
(47) Chen, Z.; Earl, P.; Americo, J.; Damon, I.; Smith, S. K.; Zhou, Y. H.; Yu, F.; Sebrell, A.; Emerson, S.; Cohen, G.; Eisenberg, R. J.; Svitel, J.; Schuck, P.; Satterfield, W.; Moss, B.; Purcell, R. *Proc. Natl. Acad. Sci. U.S.A.* **2006**, *103*, 1882.
(48) Wales, T. E.; Fadgen, K. E.; Gerhardt, G. C.; Engen, J. R. *Anal. Chem.* **2008**, *80*, 6815.
(49) van den Heuvel, R. H.; van Duijn, E.; Mazon, H.; Synowsky, S. A.; Lorenzen, K.; Versluis, C.; Brouns, S. J.; Langridge, D.; van der Oost, J.; Hoyes, J.; Heck, A. J. *Anal. Chem.* **2006**, *78*, 7473.
(50) Lorenzen, K.; versluis, C.; van Duijn, E.; van den Heuvel, R. H.; Heck, A. J. *Int. J. Mass Spectrom.* **2007**, *268*, 198.
(51) Sobott, F.; Hernandez, H.; McCammon, M. G.; Tito, M. A.; Robinson, C. V. *Anal. Chem.* **2002**, *74*, 1402.
(52) Tahallah, N.; Pinkse, M.; Maier, C. S.; Heck, A. J. *Rapid Commun. Mass Spectrom.* **2001**, *15*, 596.
(53) IGORPro, version 6.2.2.2.
(54) Gallina, A.; Bonelli, F.; Zentilin, L.; Rindi, G.; Muttini, M.; Milanesi, G. *J. Virol.* **1989**, *63*, 4645.
(55) Seifer, M.; Standring, D. N. *J. Virol.* **1994**, *68*, 5548.
(56) Hilmer, J. K.; Zlotnick, A.; Bothner, B. *J. Mol. Biol.* **2008**, *375*, 581.
(57) Schodel, F.; Moriarty, A. M.; Peterson, D. L.; Zheng, J. A.; Hughes, J. L.; Will, H.; Leturcq, D. J.; McGee, J. S.; Milich, D. R. *J. Virol.* **1992**, *66*, 106.
(58) Yoshikawa, A.; Tanaka, T.; Hoshi, Y.; Kato, N.; Tachibana, K.; Iizuka, H.; Machida, A.; Okamoto, H.; Yamasaki, M.; Miyakawa, Y.; Mayumi, M. *J. Virol.* **1993**, *67*, 6064.
(59) Malkowski, L.; Rodi, D. J.; Mandava, S.; Minh, D. L.; Gore, D. B.; Finschetti, R. F. *J. Mol. Biol.* **2008**, *375*, 529.
(60) Fricks, C. E.; Hogle, J. M. *J. Virol.* **1990**, *64*, 1934.
(61) Roivainen, M.; Piirainen, L.; Rysa, T.; Narvanen, A.; Hovi, T. *Virology* **1993**, *195*, 762.
(62) Li, Q.; Yafal, A. G.; Lee, Y. M.; Hogle, J.; Chow, M. *J. Virol.* **1994**, *68*, 3965.
(63) Lewis, J. K.; Bothner, B.; Smith, T. J.; Siuzdak, G. *Proc. Natl. Acad. Sci. U.S.A.* **1998**, *95*, 6774.
(64) Katpally, U.; Fu, T. M.; Freed, D. C.; Casimiro, D. R.; Smith, T. J. *J. Virol.* **2009**, *83*, 7040.
(65) Bothner, B.; Taylor, D.; Jun, B.; Lee, K. K.; Siuzdak, G.; Schultz, C. P.; Johnson, J. E. *Virology* **2005**, *334*, 17.
(66) Bothner, B.; Dong, X. F.; Bibbs, L.; Johnson, J. E.; Siuzdak, G. *J. Biol. Chem.* **1998**, *273*, 673.
(67) Speir, J. A.; Bothner, B.; Qu, C.; Willits, D. A.; Young, M. J.; Johnson, J. E. *J. Virol.* **2006**, *80*, 3582.
(68) Birnbaum, F.; Nassal, M. *J. Virol.* **1990**, *64*, 3319.
(69) Nassal, M. *J. Virol.* **1992**, *66*, 4107.
(70) Hatton, T.; Zhou, S.; Standring, D. N. *J. Virol.* **1992**, *66*, 5232.
(71) Roseman, A. M.; Berriman, J. A.; Wynne, S. A.; Butler, P. J.; Crowther, R. A. *Proc. Natl. Acad. Sci. U.S.A.* **2005**, *102*, 15821.
(72) Chen, C.; Wang, J. C.; Zlotnick, A. *PLoS Pathog.* **2011**, *7*, e1002388.
(73) Kaven, D.; Man, P. *Int. J. Mass Spectrom.* **2011**, *302*, 53.